

# Influence of low-frequency parameter changes on nonlinear vibro-acoustic wave modulations used for crack detection

Bin Liu<sup>1,2</sup>, Zhiwei Luo<sup>1,3</sup> and Tie Gang<sup>1</sup>

## Abstract

The use of vibro-acoustic modulation is an effective nonlinear and nondestructive approach to the detection and monitoring of cracks in fatigued, defective, and fractured materials. However, the vibro-acoustic modulation results strongly depend on choice of the testing parameters. To implement this technique for additional applications, the effect of variation in the test parameters must be well understood. This study investigates the influence of variation in the amplitude and frequency of pumping (low-frequency vibration) signals on the modulation. We apply two kinds of probing excitations, sine-wave and swept-signal excitations, and we measure the modulation intensity variation with changes in the relevant parameters to observe their influence on the modulations. Dynamic strain measurement of the crack area is utilized to analyze the relation between the degree of crack opening/closing and the modulation on the crack interface. The results indicate that the probing amplitude has little effect on the modulation, and furthermore, the sweep-signal excitation technique can be used to select the proper probing frequency. The results also indicate that there is a critical pumping strain value ( $\varepsilon_c$ ) for the crack samples. When the pumping strain reaches this critical value, the modulation reaches a maximum. However, the opening/closing area cannot increase any more even if the pumping amplitude further increases, and thus, the modulation does not change. The extent of the crack opening/closing also varies with the pumping frequency. Our results suggest that increased sensitivity to crack detection can be achieved with the use of the resonance frequency as the pumping frequency in vibro-acoustic modulation tests.

## Keywords

Vibro-acoustic modulation, parameter selection, crack opening/closing, critical pumping strain, dynamic strain

## Introduction

Vibro-acoustic modulation (VAM), also called nonlinear wave modulation spectroscopy (NWMS), is a nonlinear ultrasonic method utilized for the nondestructive testing of materials.<sup>1–3</sup> The approach detects material defects by monitoring the modulation components generated by the interaction between probing (high-frequency ultrasound  $f_0$ ) and pumping (low-frequency vibration  $f_1$ ) signals due to the nonlinear behavior arising from material damage. The method exploits the fact that these modulation components are present as a mixed frequency or sideband ( $f_0 \pm nf_1$ ) in the spectrum.

VAM is sensitive to cracks in structures even with complex geometries. In this regard, it has been reported that cracks in welded joints of large steel pipes or pipe

socket welds,<sup>2,4</sup> imperfections in diffusion bond interfaces,<sup>5</sup> and loose bolted joints<sup>6–8</sup> can be detected by means of this technique. VAM can be applied to various materials such as metal, Plexiglas, sandstone,<sup>9</sup> concrete,<sup>10,11</sup> and composites.<sup>12–14</sup> More importantly, the

<sup>1</sup>State Key Laboratory of Advanced Welding and Joining, Harbin Institute of Technology, Harbin, People's Republic of China

<sup>2</sup>Key Laboratory of Noise and Vibration Research, Institute of Acoustics, Chinese Academy of Sciences, Beijing, People's Republic of China

<sup>3</sup>Capital Aerospace Machinery Company, Beijing, People's Republic of China

## Corresponding author:

Tie Gang, State Key Laboratory of Advanced Welding and Joining, Harbin Institute of Technology, Harbin 150001, People's Republic of China.  
Email: gangt@hit.edu.cn

method does not require any highly sophisticated equipment to excite and receive signals.

Parameter selection forms one of the most important elements for test reliability. There are four main parameters in the VAM test: the amplitude and frequency of both the probing and pumping signals. The probing amplitude has little effect on the modulation between the (ultrasonic) sound and vibration on the crack interface.<sup>3,4</sup> However, the modulation effect (sensitivity) of the technique is strongly dependent on the probing ultrasonic frequency. Therefore, to make VAM more practically applicable and robust, a suitable probing frequency needs to be selected before testing. In this regard, Duffour et al.<sup>15</sup> proposed that the probing frequency should be swept over a broad range in order to lock the frequencies that yield the highest sensitivity. To quickly inspect a wide range of probing frequencies, Yoder developed a new form of probing excitation with a swept signal. Cracks in the samples were detected through the normalized modulation observed at the harmonics of the pumping frequency in the time–frequency domain.<sup>16</sup> In our previous research, we proposed a new index called  $MI_{SD}$  to evaluate the structure quality in a VAM test with swept probing excitation.<sup>17</sup>

Initial studies in this regard have shown that the ultrasound amplitude and/or phase periodically changes (modulates) because of the opening/closing of the crack interface due to vibrations.<sup>18</sup> In particular, a larger opening/closing area corresponds to a higher modulation, which indicates that the modulation intensity linearly increases with the pumping amplitude during testing.<sup>9,19</sup> The pumping frequency selection is related to the vibration mode of the structures, and thus, the sensitivity of a crack located at a certain position is different for different pumping frequencies.<sup>4</sup> In this regard, an aluminum plate was tested with different vibration modes by Klepka et al.<sup>20</sup> The relative motion mode of the crack interface in the plate was divided into three types: Mode I—opening/closing mode, Mode II—sliding mode, and Mode III—tearing mode. The test results suggested that different motion modes correspond to different modulation intensities.

This work investigates the influence of the testing parameters, particularly the low-frequency parameters, on the modulation. Two methods for probing excitation are used in this study: sine-wave excitation and swept-signal excitation. The variation in modulation with

different parameters is summarized according to the test results. Furthermore, we use dynamic strain measurement of the crack area to analyze the relation between the extent of crack opening/closing and modulation on the crack interface.

## Method and materials

### Experimental setup

Nine aluminum alloy (2024) rods with a diameter of 20 mm and length of 200 mm were tested in the experiments described in this article. Three samples (ID: #1, #6, and #7) were free of cracks, and the others were fatigue cracked in a three-point bending rig. The crack lengths along the circumferential direction of the rod were measured using an optical microscope. Table 1 lists the crack lengths of the samples. Three samples (ID: #2, #3, and #5) exhibited small cracks, and the other three samples (ID: #4, #8, and #9) exhibited large cracks (Figure 1).

The rods were supported on two foam pads during the test. Figure 2 shows the schematic representation of the experimental setup used for the VAM method. This technique needs two sets of excitations: low-frequency vibration (pumping signal  $f_1$ ) and high-frequency ultrasound (probing signal  $f_0$ ). In the setup, a shaker (HEV-20) was attached to the sample via a push rod along the direction perpendicular to its length. The pumping amplitude applied to the sample was adjusted by an amplifier. Two lead zirconate titanate (PZT) disks were bonded with epoxy glue at the ends of the rod on either side of the crack. In such a setup, each PZT transducer can be used either as a transmitter or a receiver. The input PZT disk was driven by a Rigol DG3061A signal generator. A strain gauge was bonded at the midpoint of the sample, and it was used to monitor the dynamic strain of the crack area during the VAM test. Two types of probing-frequency (high-frequency) excitations were applied during the experiment.

### Sine-wave excitation

Pure-tone sine-wave probing excitation was used to investigate the effect of the vibration parameters on the output modulation signal. The output signal was recorded with a storage oscilloscope (Rigol DS1102E) and subsequently processed and analyzed with a

**Table 1.** Fatigue crack length of Al rod.

Sample ID	#1	#2	#3	#4	#5	#6	#7	#8	#9
Crack length (mm)	0	0.7	20	42	16	0	0	33	30

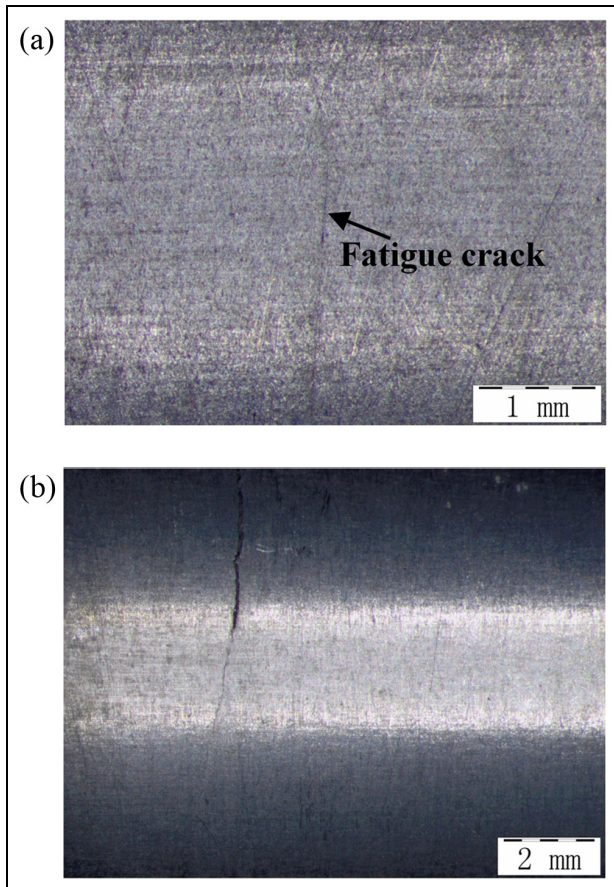


**Figure 1.** Optical detection results of (a) small-crack sample and (b) large-crack sample.

LabVIEW program. We used the modulation index  $MI_D$  proposed by Donskoy to evaluate the structure quality

$$MI_D = 20 \log_{10} \frac{A_{m-n} + A_{m+n}}{2A_m} \quad (1)$$

Here,  $A_{m \pm n}$  represents the spectral magnitude at frequency  $f_0 \pm nf_1$ , and  $A_m$  is the spectral magnitude at frequency  $f_0$ .

### Swept-signal excitation

To determine the probing frequencies that resulted in the most modulation, we used a linear sweep signal to excite the transmitter PZT disk. The output signal was processed and analyzed by a LabVIEW program. First, the high-frequency structure response (HFSR) of the sample was measured without the low-frequency vibration excitation, a Hilbert transform-based amplitude demodulation was used to obtain the HFSR envelope.

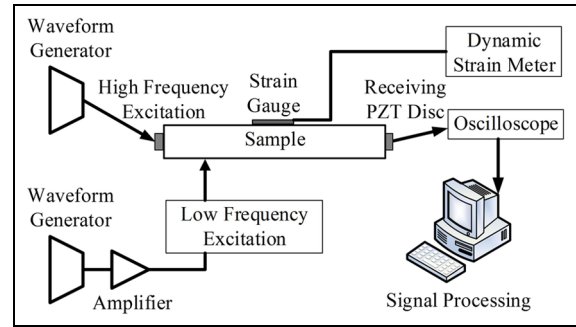


**Figure 2.** Experimental setup for vibro-acoustic modulation (VAM) testing.

Next, the low-frequency excitation was applied to the sample, and the output signal was filtered by a high-pass filter so as to separate the modulated high-frequency response from the signal. The synchronous demodulation (SD) method was used to extract the modulation information from the modulated high-frequency response.<sup>21</sup> Next, the HFSR envelope was used to normalize the signal during demodulation. The normalized envelope was transformed into the time–frequency domain with the use of the short-time Fourier transform (STFT). The modulation component could then be detected through the presence of significant energy at the harmonics of the vibration signal.

The modulation intensity of the test with swept-signal excitation can be characterized with the index  $MI_{SD}$ , which can be expressed as follows

$$MI_{SD} = S_{D1} + S_{D2} + S_{D3} + \dots \quad (2)$$

Here,  $S_{Dn}$  ( $n = 1, 2, 3, \dots$ ) denotes the energy intensity normalized by the HFSR envelope at the harmonics of the vibration frequency in the time–frequency domain result after STFT.

The nonlinear information extraction method for swept-signal excitation is different from that of sine-wave excitation, and furthermore, the  $MI_{SD}$  curve was not plotted on the dB scale in the study. In order to facilitate comparison of the test results with different excitations, the results in both cases should be consistent. In this context, a comparison of these two results<sup>17</sup> yields the following approximate relationship between  $MI_D$  and  $MI_{SD}$

$$MI_D \approx 10(\log_{10} MI_{SD} - 1) \quad (3)$$

Subsequently, the results of the VAM test with swept-signal excitation were plotted on the dB scale according to this formula.

## Results and discussion

### Selection of probing excitation

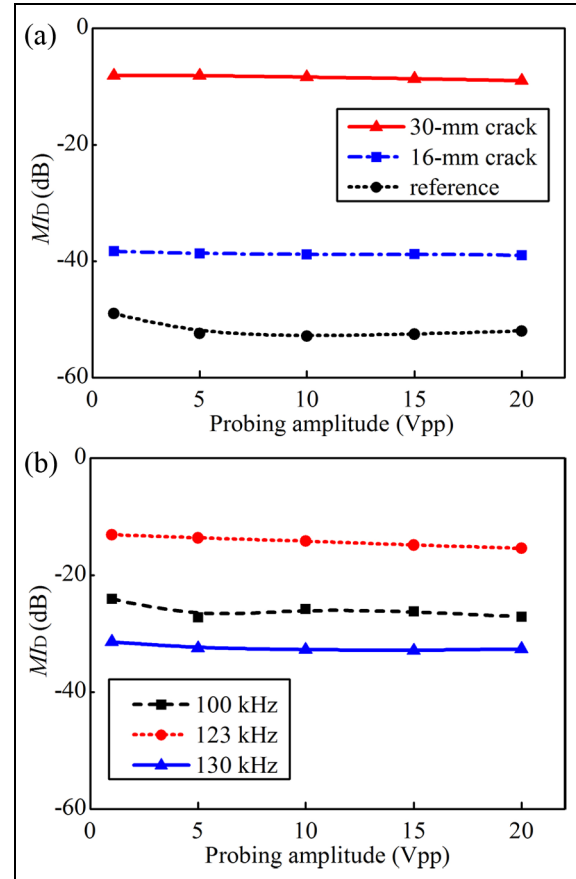
Figure 3(a) illustrates the influence of the probing amplitude on the modulation in samples with different crack sizes. The frequency of the exciting sine wave is 112 kHz with amplitudes of 1, 5, 10, 15, and 20 Vpp. The vibration force amplitude is 8 N, and the frequency is 1.5 kHz. We observe that the modulation intensity increases with increasing crack size. However, the modulation intensity remains constant with variation in the probing-signal amplitude.

Figure 3(b) depicts the influence of the probing amplitude on the modulation in sample #9 for different probing frequencies (100, 123, and 130 kHz). We note that the probing frequency significantly affects the modulation.

As mentioned above, the modulation effect (sensitivity) of the technique is strongly dependent on the probing frequency. To determine a suitable high-frequency value, we used a 90- to 140-kHz linear sweep signal with a sweep time of 500 ms and drive voltage of 20 Vpp to excite the transmitter PZT disk. All nine samples were tested, and the equivalent  $MI_D$  was calculated according to equation (3), the corresponding results are shown in Figure 4.

The  $MI_D$  value of the reference samples (Figure 4(a)) is small over the entire swept range, its average value is approximately  $-50$  dB, and there is no change as the frequency is varied. The  $MI_D$  values of the crack samples (Figure 4(b) and (c)) are significantly larger than those of the reference samples. The average values are approximately  $-40$  dB for small cracks and  $-20$  dB for large cracks. It can also be observed that the  $MI_D$  value of the crack samples varies with the probing frequency. For the small-crack samples (Figure 4(b)),  $MI_D$  varies in the range from  $-60$  to  $-20$  dB, and for large-crack samples (Figure 4(c)), the variation range of  $MI_D$  is from  $-40$  to  $0$  dB.

Another noteworthy feature is the strong modulation observed at certain frequencies for large-crack samples (Figure 4(c)), for which  $MI_D$  is  $>0$ . It implies that the sideband amplitude is larger than the probing amplitude. This “over modulation” was also observed when the pumping frequency was 1.8 kHz. The signal spectra (fast Fourier transform (FFT) with a hanning window) obtained for a probing frequency of 114.2 kHz are shown in Figure 5. The figure shows the spectra for sample #9 with the 30-mm crack, with the pumping frequency set to 1.8 kHz and pumping force set to 8 N. Here, we remark that this type of strong modulation was also observed by Zaitsev and Sas,<sup>19</sup> who attributed it to the dissipative modulation



**Figure 3.** Influence of probing amplitude on modulation for different (a) crack sizes and (b) probing frequencies (sample #9).

mechanism between the sound and vibration on the crack interface. Consequently, it is suggested that a suitable probing frequency is essential for VAM testing; otherwise, sample damage may not be correctly estimated. In this work, we chose the probing frequency to be 112 kHz.

### Pumping amplitude

Three samples (ID: #1, #5, and #9) were used to study the influence of the pumping amplitude on the modulation. The pumping force range of the shaker used in this case was 0–10 N, and its frequency was approximately 1.5 kHz. Here, we recall that modulation is caused by the crack interface opening/closing motion during the test. Therefore, in the study, we first measured the dynamic strain of the crack interface during the test. The direction of the strain gauge was set perpendicular to the crack interface, and the bond position of the reference sample corresponded to those of the crack samples. The crack opening direction was parallel

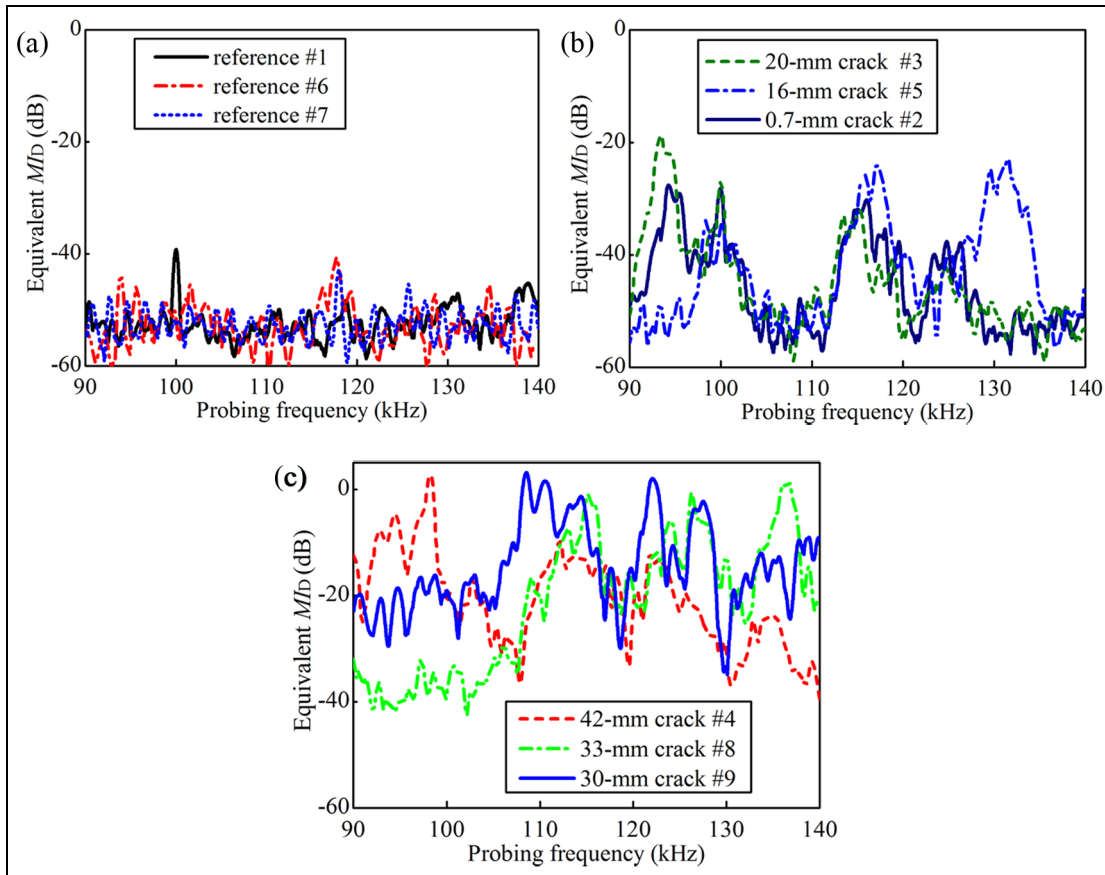


**Figure 4.** Vibro-acoustic modulation (VAM) test results obtained with swept-signal excitation of samples with (a) no defect, (b) small defect, and (c) large defect.

to the vertical plane during the test, and the strain gauge was positioned parallel to the horizontal plane.

The variation in dynamic tensile strain with pumping force amplitude at the midpoint of the samples is shown in Figure 6. The strain curve of the reference sample is represented by the dotted line (...#1), and the crack samples are represented by the dashed line (—#5, small crack) and solid line (—#9, large crack). The strain of the reference sample is less than those of the crack samples for the same amplitude. The strain is observed to increase with the crack size, and the strain of the crack samples increases drastically with an increase in the pumping amplitude.

Next, a 112-kHz, 20-V<sub>pp</sub> sine wave was chosen as the probing signal to drive the PZT disk during the VAM test. The modulation intensity of the output signal was characterized with the modulation index  $MI_D$ . Figure 7(a) shows the influence of the pumping strain (tensile strain in Figure 6) on the modulation in samples with different crack sizes. We observe that the modulation intensity of the output signal increases with the crack size. The modulation index difference between

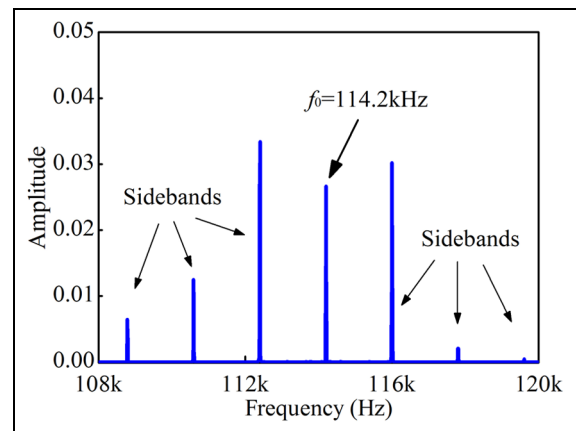


**Figure 5.** Signal spectra observed for the probing frequency of 114.2 kHz for sample #9 with 30-mm crack.

the crack sample and the reference sample can reach 45 dB. Furthermore,  $MI_D$  increases with an increase in the pumping strain. The rate of increase is comparatively rapid in the initial stage, with a subsequent

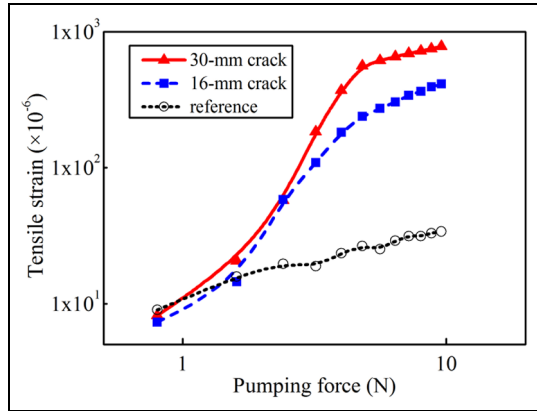


**Figure 6.** Tensile strain at crack areas as a function of the pumping force.

reduction. Furthermore, a change in the modulation index curve is observed when the strain reaches a certain value, beyond which the index does not change even when the strain further increases. The strain at the turning point is defined as the critical pumping strain ( $\epsilon_c$ ) in this work. We also note that the  $\epsilon_c$  values of the samples with different crack sizes are all different. The  $\epsilon_c$  value of sample #9 (crack length of 30 mm) is approximately  $620 \times 10^{-6}$ , whereas that of sample #5 is  $190 \times 10^{-6}$  (crack length of 16 mm).

Figure 7(b) illustrates the influence of the pumping strain on the modulation in sample #9 for different probing frequencies (100, 112, and 138 kHz) and constant values of the other exciting parameters. We observe that the  $MI_D$  curves are similar for different probing frequencies, and furthermore,  $MI_D$  remains constant when the strain reaches the critical pumping strain  $\epsilon_c$ . In addition,  $\epsilon_c$  is almost identical for the sample even at different probing frequencies, and the slopes of the  $MI_D$  curves are basically identical when the strain is less than  $\epsilon_c$ .

As per Stuin and Johnson's<sup>18</sup> assumption, the ultrasound amplitude changes at the crack interface when an opening/closing motion is generated on the interface. When the pumping strain is small, only a part of the interface will move. The opening/closing area is larger (with a resulting increase in the modulation) with greater pumping strain. Therefore, the modulation intensity linearly increases with the pumping strain in the initial stage. When the pumping strain reaches the critical value, the opening/closing motion is generated on the entire crack interface, and the modulation reaches a maximum value. However, the opening/closing area cannot increase further with further increase in pumping strain, and thus, the modulation does not change.

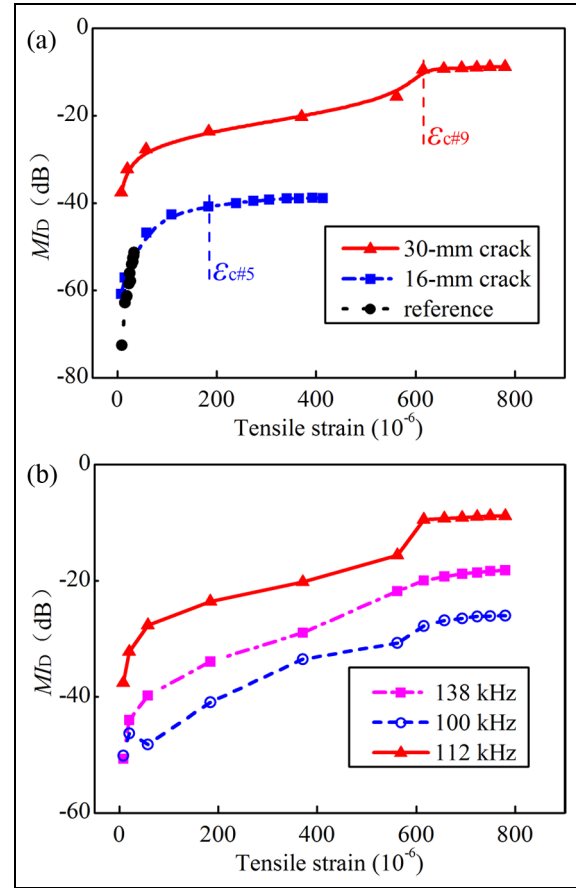


**Figure 7.** Influence of pumping strain on modulation for different (a) crack sizes and (b) probing frequencies (sample #9).

The cracks in the samples can be observed on the sample surface. According to the above analysis, when the pumping strain is small, the opening/closing motion only appears at the top part of the crack interface near the surface, but the bottom part of the crack near the tip stays closed during the test. The stronger is the pumping strain, the larger is the opening/closing area, and thus, the larger is the crack opening angle. When the pumping strain reaches the critical value, the opening/closing motion is generated along the entire crack interface including the crack tip, and the crack opening angles of samples with different crack sizes are approximately equal at their corresponding  $\epsilon_c$  values.

The  $\epsilon_c$  values of the crack samples are approximately  $190 \times 10^{-6}$  (for sample #5) and  $620 \times 10^{-6}$  (for sample #9). The projection of the crack interface on the rod cross section is assumed to be bow shaped, as shown in Figure 8. The following section demonstrates the basis of this assumption. First, the crack length ( $L$ ) around the circumference of the samples was measured by means of an optical microscope, and these results are

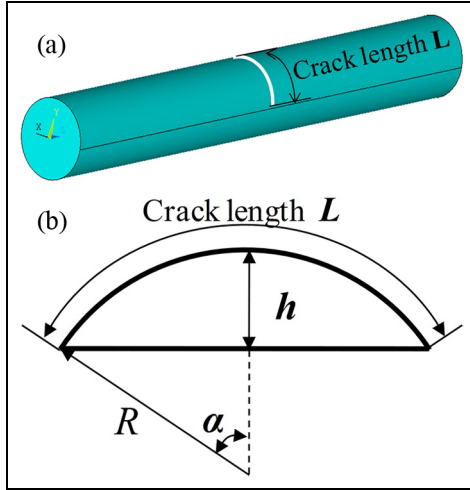


**Figure 8.** (a) Crack length measurement method and (b) simplified model of the crack area from optical measurement of the crack length.

listed in Table 1. Next, the crack depth ( $h$ ) was estimated as follows

$$h = R - R \cos \alpha$$

Here,  $R$  denotes the radius of the rod sample, and

$$\alpha = \frac{L/2}{R} \text{ (rad)}$$

Next, the crack depths of samples #5 and #9 were calculated as approximately 3 and 9.3 mm, respectively. Then, the angle  $\gamma$  between the crack walls was calculated as follows

$$\begin{aligned} \gamma_{\#5} &\approx \frac{D}{h_{\#5}} = \frac{L\epsilon_{c\#5}}{h_{\#5}} = \frac{190 \times 10^{-6} L}{3 \times 10^{-3}} \\ \gamma_{\#9} &\approx \frac{D}{h_{\#9}} = \frac{L\epsilon_{c\#9}}{h_{\#9}} = \frac{620 \times 10^{-6} L}{9.3 \times 10^{-3}} \end{aligned} \quad (4)$$

Here,  $D$  denotes the crack opening distance,  $h$  the crack depth, and  $L$  the length of the measured area.

In our study, we found that  $\gamma_{\#5} = \gamma_{\#9}$ . This implies that the opening angle of the cracks with different sizes is approximately equal at the point where the pumping strain is sufficient to “fully open” the crack interface.

According to the above analysis, the most effective approach to using ultrasound to modulate the crack interface is to set the pumping strain at least larger than the critical value, since the modulation intensity does not change with further increase in the pump amplitude. We speculate that the entire crack interface is involved in the modulation of the ultrasound vibration under this condition, and the test results yield higher-

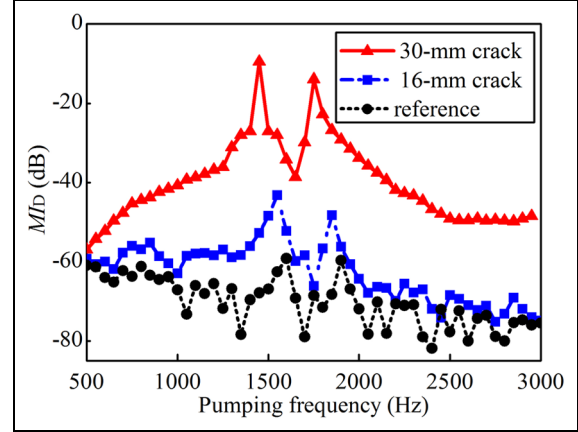


**Figure 9.** Influence of pumping frequency on modulation.

quality information about the structure. The pumping amplitude is selected as 8 N in the following test.

### Pumping frequency

The influence of the pumping frequency on the modulation in samples with different crack sizes is shown in Figure 9. The samples chosen were #1, #5, and #9, with the vibration frequency range set to 500–3000 Hz, while the other experimental parameters were identical to the corresponding ones mentioned in section “Selection of probing excitation.” The modulation intensity of the output signal was characterized with the modulation index  $MI_D$ .

The test results show that for larger crack sizes, the modulation intensity correspondingly increases. The average modulation indices of the reference sample (#1), small-crack sample (#5), and large-crack sample (#9) are  $-70.2$ ,  $-62.5$ , and  $-39.9$  dB, respectively. The modulation intensity is different at different vibration frequencies even for the same pumping amplitude, and the larger is the crack size, the larger is the difference in modulation. For example, the  $MI_D$  difference for sample #9 can reach 50 dB in the range of 500–3000 Hz, whereas this difference for sample #5 is considerably smaller.

The most prominent characteristic of the result in Figure 9 is that there are two modulation intensity peaks in the  $MI_D$  curve at specific vibration frequencies. These frequencies are approximately 1.5 and 1.8 kHz for all the samples (corresponding to modulation intensity maxima), while  $MI_D$  significantly decreases at other vibration frequencies.

Figure 10 shows the tensile strain at the midpoint of the samples for different vibration frequencies. Again, the experimental setup was identical to that described in section “Pumping amplitude.” The results show that

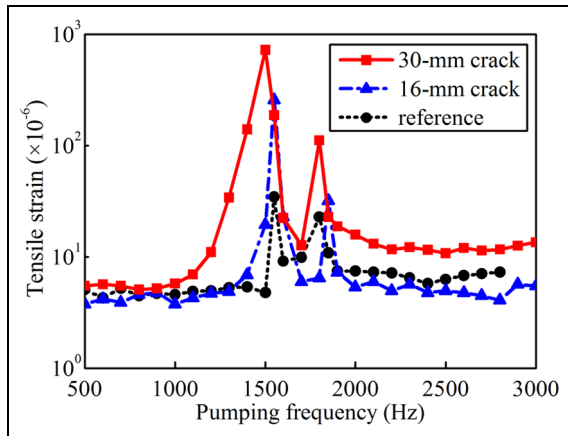


**Figure 10.** Tensile strain of crack interface for different pumping frequencies.

for the same pumping frequency, the larger is the crack size, the higher is the strain. The strain curve is similar to the  $MI_D$  curve shown in Figure 9. The frequencies corresponding to the strain peaks of the samples are the resonance frequencies of the samples under the experimental conditions.

It can also be determined that the strain at 1.5 kHz is larger than that at 1.8 kHz. In addition, the strains of the crack samples are significantly larger than that of the reference sample at the corresponding resonance frequencies even with the same vibration force amplitude, but the difference among these strains decreases at non-resonant frequencies. Upon comparing these results with those in Figure 9, we speculate that the larger is the strain (extent of crack opening), the larger is the modulation intensity.

Based on the results of the VAM test and dynamic strain measurements, we speculate that the crack opening/closing extent varies with the pumping frequency, thus modulating the amplitude and/or phase of the ultrasound passing through the crack interface. The larger is the crack opening/closing, the stronger is the modulation of the probing signal. Furthermore, for the same pumping amplitude, a larger degree of crack opening/closing can be achieved by selecting a suitable pumping frequency.

## Conclusion

In this VAM study, we discussed the principle and method of selecting the parameters for the VAM test (particularly the low-frequency parameter), and we analyzed the manner in which the parameters affect the modulation. The results demonstrated that probing amplitude has little effect on the modulation, and a suitable probing frequency can be quickly selected with the use of the sweep-signal excitation technique.

The results indicate that there is a critical pumping strain ( $\varepsilon_c$ ) for the crack samples. The modulation intensity increases with the pumping strain in the initial stage because the degree of crack opening/closing also correspondingly increases. When the strain reaches the critical value, the entire crack interface is involved in the modulation of the ultrasound by vibration, and the modulation reaches a maximum. However, the opening/closing area cannot increase further with further increase in the pumping strain, and thus, the modulation does not change. This fact can be used to determine the proper pumping strain and to carry out a preliminary assessment of the crack size.

Our results also demonstrated that the degree of crack opening/closing also varies with the pumping frequency. It increases significantly when the pumping frequency is close to the resonance frequency of the structure, which causes strong modulation at the interface. Thus, the choice of the resonant frequency as the pumping frequency makes the method more sensitive to crack detection.

However, the reason as to why the modulation intensity strongly depends on the probing frequency is not clear thus far. Furthermore, we do not know whether the modulation distribution in the probing-frequency range is governed by a law or principle. In addition, we do not know the factors that influence this distribution law. These questions will need to form the focus of future researches.

## Acknowledgements

The authors thank Dr Li Shuqi and Dr Cui Wei (State Key Laboratory of Advanced Welding and Joining, Harbin Institute of Technology) for their help with the dynamic strain measurements. They also thank the anonymous reviewers for their useful suggestions.

## Funding

The author(s) disclosed receipt of the following financial support for the research, authorship, and/or publication of this article: This work was supported by the National Natural Science Foundation of China 51575134, 51175113, and 51105033.

## References

1. Jhang KY. Nonlinear ultrasonic techniques for nondestructive assessment of micro damage in material: a review. *Int J Precis Eng Man* 2009; 10(1): 123–135.
2. Donskoy DM and Sutin AM. Vibro-acoustic modulation nondestructive evaluation technique. *J Intel Mat Syst Str* 1998; 9(9): 765–771.
3. Van Den Abeele KE, Johnson PA and Sutin A. Nonlinear elastic wave spectroscopy (NEWS) techniques to discern material damage, part I: nonlinear wave



- modulation spectroscopy (NWMS). *Res Nondestruct Eval* 2000; 12(1): 17–30.
4. Donskoy D, Sutin A and Ekimov A. Nonlinear acoustic interaction on contact interfaces and its use for nondestructive testing. *NDT&E Int* 2001; 34(4): 231–238.
  5. Escobar-Ruiz E, Ruiz A, Hassan W, et al. Non-linear ultrasonic NDE of titanium diffusion bonds. *J Nondestruct Eval* 2014; 33(2): 187–195.
  6. Meyer JJ and Adams DE. Theoretical and experimental evidence for using impact modulation to assess bolted joints. *Nonlinear Dynam* 2015; 81(1–2): 103–117.
  7. Amerini F and Meo M. Structural health monitoring of bolted joints using linear and nonlinear acoustic/ultrasound methods. *Struct Health Monit* 2011; 10(6): 659–672.
  8. Jaques JL, Adams DE, Doyle D, et al. Experimental study of impact modulation for quantifying loose bolt torque in on-demand satellites. In: *Proceedings of the ASME 2010 conference on smart materials, adaptive structures and intelligent systems*, Philadelphia, PA, 28 September–1 October 2010, pp. 727–734. New York: ASME.
  9. Van Den Abeele KE, Sutin A, Carmeliet J, et al. Micro-damage diagnostics using nonlinear elastic wave spectroscopy (NEWS). *NDT&E Int* 2001; 34(4): 239–248.
  10. Chen J, Jayapalan AR, Kim JY, et al. Nonlinear wave modulation spectroscopy method for ultra-accelerated alkali-silica reaction assessment. *ACI Mater J* 2009; 106(4): 340–348.
  11. Warnemuende K and Wu HC. Actively modulated acoustic nondestructive evaluation of concrete. *Cement Concrete Res* 2004; 34(4): 563–570.
  12. Klepka A, Pieczonka L, Staszewski WJ, et al. Impact damage detection in laminated composites by non-linear vibro-acoustic wave modulations. *Compos Part B: Eng* 2014; 65: 99–108.
  13. Pieczonka L, Klepka A, Staszewski WJ, et al. Analysis of vibro-acoustic modulations in nonlinear acoustics used for impact damage detection—numerical and experimental study. *Key Eng Mat* 2013; 558: 341–348.
  14. Meo M, Polimeno U and Zumpano G. Detecting damage in composite material using nonlinear elastic wave spectroscopy methods. *Appl Compos Mater* 2008; 15(3): 115–126.
  15. Duffour P, Morbidini M and Cawley P. A study of the vibro-acoustic modulation technique for the detection of cracks in metals. *J Acoust Soc Am* 2006; 119(3): 1463–1475.
  16. Yoder NC and Adams DE. Vibro-acoustic modulation utilizing a swept probing signal for robust crack detection. *Struct Health Monit* 2010; 9(3): 257–267.
  17. Liu B, Gang T, Wan C, et al. Analysis of nonlinear modulation between sound and vibrations in metallic structure and its use for damage detection. *Nondestruct Test Eva* 2015; 30(3): 277–290.
  18. Sutin AM and Johnson PA. Nonlinear elastic wave NDE II: nonlinear wave modulation spectroscopy and nonlinear time reversed acoustics. *AIP Conf Proc* 2005; 760: 385–392.
  19. Zaitsev V and Sas P. Nonlinear response of a weakly damaged metal sample: a dissipative modulation mechanism of vibro-acoustic interaction. *J Vib Control* 2000; 6(6): 803–822.
  20. Klepka A, Staszewski WJ, Jenal RB, et al. Nonlinear acoustics for fatigue crack detection—experimental investigations of vibro-acoustic wave modulations. *Struct Health Monit* 2012; 11(2): 197–211.
  21. Sohn H, Lim HJ, DeSimio MP, et al. Nonlinear ultrasonic wave modulation for online fatigue crack detection. *J Sound Vib* 2014; 333(5): 1473–1484.